Brain Structure and Function (2020) 225:1123–1133
https://doi.org/10.1007/s00429-020-02064-z

ORIGINAL ARTICLE

Altered brain white matter connectome in children and adolescents with prenatal alcohol exposure

Xiangyu Long[1,2,3] · Graham Little[4] · Sarah Treit[4] · Christian Beaulieu[4] · Gaolang Gong[5,6] · Catherine Lebel[1,2,3]

Received: 7 September 2019 / Accepted: 24 March 2020 / Published online: 1 April 2020

Abstract

Diffuson tensor imaging (DTI) has demonstrated widespread alterations of brain white matter structure in children with prenatal alcohol exposure (PAE), yet it remains unclear how these alterations affect the structural brain network as a whole. The present study aimed to examine changes in the DTI-based structural connectome in children and adolescents with PAE compared to unexposed controls. Participants were 121 children and adolescents with PAE (51 females) and 119 typically-developing controls (49 females) aged 5–18 years with DTI data collected at one of four research centers across Canada. Graph-theory based analysis was performed on the connectivity matrix constructed from whole-brain white matter fibers via deterministic tractography. The PAE group had significantly decreased whole-brain global efficiency, degree centrality, and participation coefficients, as well as increased shortest path length and betweenness centrality compared to unexposed controls. Individuals with PAE had decreased connectivity between the attention, somatomotor, and default mode networks compared to controls. This study demonstrates decreased structural white matter connectivity in children and adolescents with PAE at a whole-brain level, suggesting widespread alterations in how networks are connected with each other. This decreased connectivity may underlie cognitive and behavioural difficulties in children with PAE.

Keywords Prenatal alcohol exposure · Diffusion tensor imaging · Graph theory · Structural connectome · Global efficiency · Inter-/intra-network

Introduction

Drinking alcohol during pregnancy is relatively common worldwide (~ 10% of pregnant women report consuming alcohol) (Lange et al. 2017a; Popova et al. 2017), and prenatal alcohol exposure (PAE) is associated with cognitive difficulties, impaired attention, motor deficits, and/or memory and language problems in children (Jacobson and Jacobson 2002; Mukherjee et al. 2006; Rasmussen et al. 2008, 2013; Riley et al. 2011; Doney et al. 2014; Lange et al. 2017b). Over the past two decades, neuroimaging studies have shown that PAE can also result in a variety of alterations to brain structure, including smaller brain volumes, thinner cortex, and malformations of the corpus callosum (Riley et al. 2004, 2011; Wozniak et al. 2006; Norman et al. 2009; Lebel et al. 2011; Wozniak and Muetzel 2011; Moore et al. 2014; Donald et al. 2015; Drew and Kane 2015; Zhou et al. 2017; Nguyen et al. 2017). Using diffusion tensor imaging (DTI), a number of studies have revealed widespread alterations to white matter microstructure, including lower fractional anisotropy (FA) and/or higher mean diffusivity (MD) in

Electronic supplementary material The online version of this article (https://doi.org/10.1007/s00429-020-02064-z) contains supplementary material, which is available to authorized users.

✉ Catherine Lebel
clebel@ucalgary.ca

1 Department of Radiology, University of Calgary, Calgary, AB, Canada

2 Alberta Children's Hospital Research Institute, B4-513, University of Calgary, 2888 Shaganappi Trail, Calgary, NWAB T3B 6A8, Canada

3 Hotchkiss Brain Institute, University of Calgary, Calgary, AB, Canada

4 Department of Biomedical Engineering, University of Alberta, Edmonton, AB, Canada

5 State Key Laboratory of Cognitive Neuroscience and Learning & IDG, McGovern Institute for Brain Research, Beijing, China

6 Beijing Key Laboratory of Brain Imaging and Connectomics, Beijing Normal University, Beijing, China

callosal, limbic, projection, and association white matter tracts in children and adults with PAE (Ma et al. 2005; Wozniak et al. 2006; Lebel et al. 2008; Sowell et al. 2008; Li et al. 2009; Fryer et al. 2009; Santhanam et al. 2011; Treit et al. 2014, 2017; Fan et al. 2015; Paolozza et al. 2017). These widespread alterations suggest that large-scale brain networks may be affected by PAE, but it remains unclear whether topological features and connectivity among networks are altered in individuals with PAE.

Graph-theory analysis is a powerful tool to investigate the complex brain network at a global level (Bassett and Bullmore 2006; Bullmore and Sporns 2009; Park and Friston 2013). By constructing a whole brain connectome from the region-to-region white matter connectivity, graph theory analysis measures the mathematical features of the connectome (Iturria-Medina et al. 2007, 2008; Gong et al. 2009). One of the important features of the human brain network is its small-worldness. Small-world networks show high efficiency and high local connectivity, enabling efficient communication over both short and long distances (Bassett and Bullmore 2006; Bullmore and Sporns 2009; Gong et al. 2009). Graph-theory analysis using DTI has been applied broadly in the neuroimaging field to better understand brain development from infancy to adulthood (Chen et al. 2013; Huang et al. 2015), as well as to identify alterations in neurodevelopmental disorders including attention deficit hyperactivity disorder, autism and Turner syndrome (Cao et al. 2013; Rudie et al. 2013; Fornito et al. 2015; Sidlauskaite et al. 2015; Zhao et al. 2018). Therefore, such complex network analysis may provide more insight into the whole-brain structural alterations associated with PAE.

Two previous PAE studies investigated the brain's functional connectome using resting-state functional MRI (Wozniak et al. 2013, 2017). One study found children and adolescents with PAE ($n = 24$, aged 10–17 years) had significantly increased shortest path length and decreased global efficiency than unexposed controls (Wozniak et al. 2013). The other study ($n = 75$, 7–17 years, non-overlapping with previous sample) found no significant differences in global graph theoretic measures, but did find higher variability of the gragh theoretic measures in the PAE group compared to controls (Wozniak et al. 2017). It is likely that structural network alterations underlie these functional connectome abnormalities, though the nature of the structural brain connectome in children with PAE is still unclear. Only one previous study examined the brain's structural connectome in neonates with PAE using DTI, showing similar whole-brain structural metrics to unexposed controls (Roos et al. 2018). The purpose of this study was to examine the structural connectome in children and adolescents with PAE using DTI-based network analysis. Based on previous findings of widespread decreased white matter volume and FA (Lebel et al. 2011; Wozniak and Muetzel 2011), we hypothesized that the structural network of children and adolescents with PAE would have lower network efficiency and degree centrality compared to unexposed controls.

Methods and materials

Participants

This study combines data from the following two research cohorts (Table 1):

1. The Kids Brain Health Network (KBHN, previously NeuroDevNet) FASD cohort (Reynolds et al. 2011), which collected data on 186 participants aged 5–18 years (91 with PAE; 95 unexposed controls). Participants received MRI scans at one of four research sites across Canada: University of Alberta (UofA), Edmonton, Alberta; Queen's University (QU), Kingston, Ontario; University of Manitoba (UofM), Winnipeg, Manitoba; and University of British Columbia (UBC), Vancouver, BC. This sample overlaps with that in a previously published DTI study of PAE (Paolozza et al. 2017). Participants with PAE were recruited from FASD diagnostic clinics within the participating cities. Controls were recruited from the same geographic regions by each site using advertisements in print and online.
2. The Canadian Institutes of Health Research (CIHR) FASD project (Lebel et al. 2008), which recruited 144 participants aged 5–32 years (70 with PAE and 74 unexposed controls). Participants with PAE were recruited from the FASD diagnostic clinic at the Glenrose Rehabilitation Hospital and via school and social work services in Edmonton, Alberta, Canada. Participants received MRI scans at the University of Alberta, Edmonton, Canada. This sample overlaps with samples in previously published DTI studies of PAE (Lebel et al. 2008, 2010; Treit et al. 2013, 2017; Green et al. 2013).

The inclusion criterion for PAE participants in both studies was confirmed PAE and/or a diagnosis of fetal alcohol spectrum disorder (FASD). Only the age ranges varied between studies: KBHN: 5 to 18 years, CIHR: 5 to 32 years. Exclusion criteria for both studies for both controls and individuals with PAE were contraindications to MRI, neurological disorders, and head injury. We limited the current analysis to children and adolescents (≤ 18 years). From the original sample of 330 participants, a total of 90 participants were excluded due to: age (> 18 years: PAE = 10, Control = 10), no T1-weighted data (PAE = 2, Control = 2), or poor data quality (e.g.,

Table 1 Demographics of the prenatal alcohol exposure (PAE) and control groups across two cohorts (The Kids Brain Health Network, KBHN and the Canadian Institutes of Health Research, CIHR) and sites

Cohort	Site	Group	*N*	Age (years)	Sex (F/M)	Ethnicity (First nations/Caucasian/other)
KBHN	University of Alberta	PAE	20	11.6 ± 3.2	9/11	14/3/3*
		Controls	14	10.6 ± 3.1	5/9	1/12/1
	Queen's University	PAE	23	11.8 ± 3.4	11/12	4/15/4
		Controls	15	12.7 ± 4.2	7/8	0/15/0
	University of Manitoba	PAE	11	12.9 ± 1.4	5/6	5/1/5*
		Controls	10	10.8 ± 2.7	3/7	0/10/0
	University of British Columbia	PAE	15	11.9 ± 4.7	5/10	10/4/1*
		Controls	18	12.9 ± 2.3	4/14	0/13/5
CIHR	University of Alberta	PAE	52	12.2 ± 3.0	21/31	17/15/20*
		Controls	62	11.4 ± 3.1	30/32	2/51/9
Total		PAE	121	12.0 ± 3.3	51/70	50/38/33*
		Controls	119	11.6 ± 3.2	49/70	3/101/15

*Significant group differences (PAE vs controls) within each subgroup at $p < 0.05$. Two-sample *t*-tests were performed for age; Chi-square tests were performed for sex and ethnicity. Only ethnicity was significantly different at three sites in the KBHN cohort (University of Alberta: Chi-square = 17.14, $p = 0.00019$; University of Manitoba, Chi-square = 13.35, $p = 0.0013$; University of British Columbia: Chi-square = 14.45, $p = 0.00073$) and the CIHR cohort (Chi-square = 35.04, $p < 1 \times 10^{-5}$), as well as between the PAE and control groups combined across sites (Chi-square = 76.97, $p < 1 \times 10^{-5}$)

poor whole-brain coverage, poor T1 or severe distortion of images by visual inspection; PAE = 29, Control = 37). Thus, the final sample analyzed DTI data from 121 children and adolescents with PAE and 119 unexposed controls, ranging from 5 to 18 years (Table 1).

Control participants had no self-reported neurological, psychiatric, and developmental disorders. Informed consent was obtained from a parent or guardian, and assent was obtained from each child before scanning. This study was approved by the local health research ethics committee for each research facility. In the PAE group, participants from the KBHN cohort had been previously diagnosed according to the Canadian Guidelines for FASD diagnosis (Chudley et al. 2005) or had confirmed PAE from a credible source (Paolozza et al. 2017). In the CIHR cohort, PAE was confirmed by the local hospital FASD clinic or a community physician (Lebel et al. 2008). Of the 69 participants with PAE in the KBHN cohort, 27 were diagnosed with alcohol-related neurodevelopmental disorder, 13 with partial fetal alcohol syndrome, and 5 with fetal alcohol syndrome. These diagnoses all fall under the FASD umbrella. 24 participants in the KBHN cohort had confirmed PAE but no specific diagnosis under the FASD umbrella. Of the 52 participants with PAE in the CIHR cohort, 30 were diagnosed with alcohol-related neurodevelopmental disorder, 4 with partial fetal alcohol syndrome, 12 with fetal alcohol syndrome, and 6 had confirmed PAE but no specific diagnosis under the FASD umbrella.

MRI acquisition

For the KBHN cohort, MRI data were acquired at each site with closely matched protocols on a 1.5 T Siemens Sonata at UofA, 3 T Siemens Trio at QU and UofM, and 3 T Philips Intera at UBC. The parameters for T1-weighted structural images were axial MPRAGE, UofA: TR = 2180 ms, TE = 4.38 ms; QU/UofM: TR = 2180 ms, TE = 3.45 ms; UBC: TR = 1858 ms, TE = 3.6 ms, and common flip angle = 15°, 160 slices, voxel size = $1 \times 1 \times 1$ mm^3, matrix size = 256×192 (256×256 for UBC). Common parameters of DTI dataset across four sites were as follows: dual spin-echo echo planar sequence, 1 average, voxel size = $2.2 \times 2.2 \times 2.2$ mm^3, 50 axial slices with no gap, matrix size = 96×96; 30 gradient directions, $b = 1000$ s/mm^2, 1 (UBC, UofM, QU) or 5 (UofA) b0 images, TR = 7700 ms (UofA), 6828 ms (UBC) or 6600 ms (UofM, QU), TE = 94 ms (QU, UofM and UofA) or 69 ms (UBC), scan time = 3: 45 (UBC, QU, UofM) or 4:39 min (UofA) (Paolozza et al. 2017).

For the CIHR cohort, the MRI images were collected from the same 1.5 T Siemens Sonata scanner at UofA, but using a different protocol. T1-weighted structural images were collected using an MPRAGE sequence with TR = 1870 ms, TE = 4.38 ms, 144 slices, interpolated voxel size = $0.5 \times 0.5 \times 1$ mm^3, matrix size = 383×510; DTI scan parameters were the following: dual spin-echo echo planar sequence with 8 averages, voxel size = $1.7 \times 1.7 \times 3$ mm^3 zero-filled to $0.86 \times 0.86 \times 3$ mm^3, 40 axial slices with

no gap, matrix size = 256 × 256; 6 gradient directions, $b = 1000$ s/mm^2, 1 b0 image, 8 averages, TR = 6400 ms, TE = 88 ms, scan time = 4:29 min (Lebel et al. 2008, 2010).

MRI data preprocessing

Structural T1 data were skull-stripped and segmented into gray matter, white matter, and cerebrospinal fluid using FSL version 5.0.9 (Zhang et al. 2001; Jenkinson et al. 2012). Total brain volume was calculated as the sum of gray matter and white matter volumes, and used as a covariate for the group comparison analysis because it is consistently decreased in the PAE (Lebel et al. 2011; Treit et al. 2016, 2017; Jarmasz et al. 2017; Nguyen et al. 2017), and can affect graph measurements (Yan et al. 2011; Li et al. 2015). DTI data were preprocessed in ExploreDTI version 4.8.6 (Leemans et al. 2009), including corrections for Gibbs ringing, head motion, and eddy current distortions, followed by calculation of the diffusion tensor to yield fractional anisotropy and mean diffusivity per voxel. Deterministic tractography of the whole brain was performed using the following parameters: seedpoint resolution = 2 × 2 × 2 mm^3, seed FA threshold = 0.15, fiber length range = 50–500 mm, angle threshold = 30°, step size = 1, linear interpolation. Individual FA maps were co-registered to a FA template (FMRIB58_FA_1mm.nii.gz) in standard MNI space using FLIRT in FSL (Jenkinson and Smith 2001; Jenkinson et al. 2002), and the affine transformation matrix was saved for subsequent analysis.

Structural connectome analysis

To build the individual DTI-based structural connectivity matrices, the Automated Anatomical Labeling (AAL) template was used to subdivide the brain into 90 regions excluding the cerebellum (Tzourio-Mazoyer et al. 2002; Bullmore and Sporns 2009). The AAL template in MNI space was provided by MRIcron (Rorden and Brett 2000). Individual level AAL templates were created by transforming the standard AAL template from MNI space to individual DTI space through the affine transformation matrix calculated above. The individual AAL template was dilated with a 3-mm radius sphere using the FSL command "fslmaths" to make sure all AAL regions were reached by fiber tracts. Individual AAL template and whole-brain fiber tractography were input to the ExploreDTI toolbox to create a 90 × 90 region-wise connectivity matrix for each individual with "PASS" option, which means two regions were considered connected even if a third region was passed through (Sidlauskaite et al. 2015; Dimond et al. 2017). Each element of the matrix contained the averaged FA value within the connected fiber tracts between regions and was set to zero if there was no connection. All connectivity matrices were fully connected. The intensity of the connectome was calculated by averaging all elements in the weighted matrix. The connectome density was calculated as the ratio between the number of existing edges and the size of the matrix. The weighted connectivity matrix was binarized to 1 and 0 for the calculations of the graph theoretical metrics (Fig. 1).

Graph theoretical metrics (clustering coefficient, shortest path length, small-worldness (i.e., λ, γ and σ), local efficiency, global efficiency, betweenness centrality and degree centrality) were calculated from each individual connectivity matrix using the GRETNA toolbox (Wang et al. 2015). Clustering coefficient measures the connection density among all neighbors of each node; shortest path length is the lowest number of pathways necessary to transfer information between any pair of nodes in the graph; local efficiency measures the efficiency of transferring information in a graph of each node and its neighbors based on the inverse of shortest path length; global efficiency (or nodal efficiency) is the efficiency of a node to all other nodes in the whole graph; betweenness centrality measures the number of shortest pathways that pass through each node; degree centrality measures the number of the connections of each node to the rest of the network (Humphries et al. 2006; Bassett and Bullmore 2006; Bullmore and Sporns 2009; Buckner et al. 2009; Rubinov and Sporns 2010; Wang et al. 2010; Cao et al. 2013; Power et al. 2013). Small-worldness analysis used 100 randomly-generated networks (Maslov and Sneppen 2002): λ measures the ratio between the real shortest path length and that of the random networks; γ measures the ratio between the real clustering coefficient and that of the random networks; σ (small-worldness) is the ratio between λ and γ. The whole-brain averaged metrics are the mean of each metric across all nodes of the graph.

Permutation tests on the connectome average intensity, average density, whole brain and nodal metrics were used

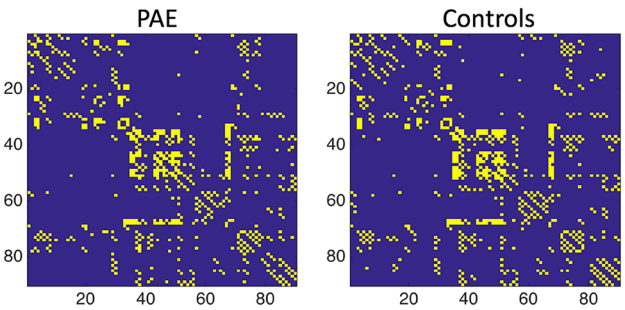

Fig. 1 The group-averaged binarized connectivity matrix of prenatal alcohol exposure (PAE) group and unexposed controls. Each row/column represents an automated anatomical labeling (AAL) region with the same order provided in MRIcron (Rorden and Brett 2000). Yellow in the matrix represents a connection between a pair of AAL regions, while blue means no connection was present. An arbitrary threshold (= 1) was applied to the matrix for viewing purposes

to test for differences between the PAE and control groups controlling for age, sex, total brain volume, scan site, cohort (KBHN or CIHR), and ethnicity (First nation/Caucasian/Other). Results are shown both uncorrected and corrected for multiple comparisons using the false discovery rate (FDR) correction. For nodal metrics, significance was set to $p < 0.05$ with FDR correction applied to account for the high number of nodes across the brain. These tests were performed in the GRETNA toolbox (Wang et al. 2015). A supplementary analysis was performed in the same manner as above, but without controlling for total brain volume.

Supplementary analyses were also performed to examine interactions between group and sex and group and age. Finally, as an additional test of age-related differences, participants were divided into three separate age bins and group differences were tested as above.

To examine separate brain networks, the 90 AAL regions were clustered based on the seven networks described in (Yeo et al. 2011): the visual, somatomotor, dorsal attention, ventral attention, limbic, frontoparietal, and the default mode networks. The bilateral caudate, putamen, pallidum, and thalamus were clustered to form an eighth network named the deep gray matter network (Baum et al. 2017). Interactions (i.e., total number of edges) between (28 comparisons) and within (8 comparisons) these networks, and the participation coefficient based on the network parcellation, were calculated and compared between groups with permutation tests controlling for covariates mentioned previously. Results are reported both uncorrected and after FDR correction for multiple comparisons.

Results

Group differences on the whole brain metrics

The PAE group had significantly decreased total brain volume (difference = 5.07%, $t = -4.00$, $p < 8.50 \times 10^{-5}$), averaged connectome intensity (difference = 4.42%, $t = -2.86$, $p = 0.005$), and connectome density (difference = 3.78%, $t = -3.16$, $p = 0.002$) compared to controls.

Table 2 shows group comparisons on the whole-brain averaged metrics. Global efficiency, degree centrality, and participation coefficient were all lower in the PAE group than controls. Shortest path length and betweenness centrality were higher in the PAE group compared to controls.

No differences at the nodal level remained significant after FDR corrections at $p < 0.05$.

Supplementary analyses

Group differences remained similar when whole brain volume was not controlled (Supplementary Table 1). No significant group-by-sex (Supplementary Table 2) or group-by-age (Supplementary Table 3) interactions were significant before or after FDR correction for multiple comparisons. Group differences in age subgroups are provided in Supplementary Table 4.

Differences in network interactions

The number of connections among networks was decreased in the PAE group compared to controls (Fig. 2), with the differences in connections between the default mode and somatomotor networks and between the ventral attention and somatomotor networks surviving FDR correction. The somatomotor and the ventral attention network also had reduced intra-network connectivity in the PAE group (uncorrected).

Discussion

In a large cohort of children and adolescents with PAE, we show decreased global efficiency, degree centrality, and participation coefficient, as well as increased shortest path

Table 2 Group differences for whole-brain averaged metrics

	PAE ($n = 121$)	Controls ($n = 119$)	Permutation p-value	% Difference
Clustering coefficient	0.70 ± 0.03	0.70 ± 0.02	0.08	0.91
Shortest path length	1.39 ± 0.04	1.37 ± 0.04	0.03	1.27
λ	1.22 ± 0.08	1.20 ± 0.08	0.18	1.48
γ	1.01 ± 0.00	1.00 ± 0.00	0.19	0.07
σ	1.22 ± 0.08	1.22 ± 0.07	0.17	1.41
Local efficiency	0.85 ± 0.01	0.85 ± 0.01	0.08	0.38
Global efficiency	0.72 ± 0.02	0.73 ± 0.02	0.03	1.27
Betweenness centrality	25.34 ± 2.36	24.43 ± 2.28	0.04	3.63
Degree centrality	40.34± 3.84	41.89 ± 3.77	0.03	3.78
Participation coefficient	0.95 ± 0.007	0.95 ± 0.01	0.01	0.25

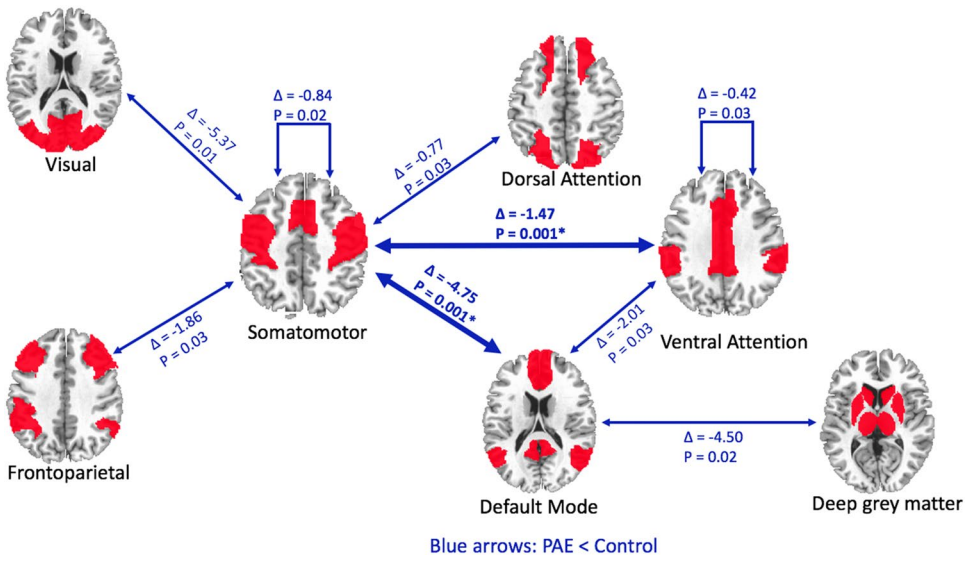

Fig. 2 The prenatal alcohol exposure (PAE) group had widely reduced inter-network connectivity. Blue indicates lower connectivity in the PAE group compared to unexposed controls, with arrows indicating reduced interactions between and within networks. Under each network/interaction with significant group differences, the mean difference between number of connections and uncorrected *p*-values are given. Bold arrows and asterisks indicate $p < 0.05$ after false discovery rate (FDR) correction for multiple comparisons

length and betweenness centrality for the first time. Furthermore, interactions between three networks were significantly weaker in the PAE group. This provides evidence of a disrupted structural connectome in PAE, suggesting that widespread global alterations to the brain's structural networks are present in children and adolescents following prenatal exposure to alcohol.

Altered connectome measures in PAE

Structural connectome features were altered in children and adolescents with PAE, both on a global level and in the network interactions. These findings align well with the two previous studies of the brain's connectome in PAE, both of which examined functional connectivity (Wozniak et al. 2013, 2017). One study showed increased shortest path length and decreased global efficiency in the PAE group compared to controls (Wozniak et al. 2013), and the other study found higher variability of network measurements in the PAE group (Wozniak et al. 2017). Both of these resting-state fMRI studies found that the PAE group had similar small-worldness (σ) to unexposed controls. Structural connectivity provides the anatomical basis of functional connectivity between brain areas. Previous studies have shown high agreement of strength and spatiality between structural and functional connectomes (Skudlarski et al. 2008; Honey et al. 2009, 2010; Hermundstad et al. 2013; Horn et al. 2014), but have also found that regions with high functional connectivity may not have direct structural connectivity (Hagmann et al. 2008; Honey et al. 2009). Graphic measures such as network hubs and small-worldness tend to share similar features between white matter-based structural networks and resting-state functional networks (Bassett and Bullmore 2006; Honey et al. 2010). Our results show similar small-worldness in both groups, and increased shortest path length, and lower global efficiency in the PAE group, in agreement with these functional connectome studies.

Nodal level metrics were not significantly different between groups. Previous studies found that the connections among nodes shift from a more local to a more distributed arrangement from early childhood to adulthood (Fair et al. 2008, 2009; Power et al. 2010), suggesting that the lack of differences here may be related to the wide age range, while inconsistencies between studies likely relate to developmental stage. A previous DTI-based connectomic study found decreased shortest path length and increased local efficiency from early childhood to adolescence in unexposed controls (Chen et al. 2013), which were in line with the present study (Supplementary Table 3). However, interactions between group and age for the whole-brain averaged graphic measures were not significant, nor were there differences when participants were grouped by age and each age range was tested separately (Supplementary Tables 3 and 4). This suggests few changes in the nodal structural development in the age range used here, but rather that the network is altered at a global level. This agrees well with previous research showing widespread structural brain alterations rather than striking focal changes in children and adolescents with PAE (Riley et al. 2004; Lebel et al. 2011; Wozniak et al. 2013; Nguyen et al. 2017). More subtle changes at individual nodes and edges may ultimately lead to the alterations at the whole network level.

Increased shortest path length and lower global efficiency might reflect the fact that a graph with fewer edges needs more pathways to connect pairs of nodes (Achard and Bullmore 2007; Markov et al. 2011). We found that the connectivity matrices of children and adolescents with PAE were less dense, which likely reflects the weaker white

matter fiber connectivity as evidenced by lower FA found in previous studies (Wozniak et al. 2006; Lebel et al. 2008, 2011; Wozniak and Muetzel 2011; Treit et al. 2013). Local connectivity, including the clustering coefficient and local efficiency metrics, was similar in children with PAE and controls. Thus, the structural connectome of children and adolescents with PAE seems to have slightly less of a small-world network arrangement than unexposed controls, with slight shifts toward a more regular network arrangement. A regular network is a network in which nodes only connect to their neighbors, with no long-range connection and low global efficiency compared to the optimal small-world network structure (Watts and Strogatz 1998; Bassett and Bullmore 2006; Bullmore and Sporns 2009).

Decreased inter- and intra-network connectivity in PAE

We employed a widely used functional network segregation model to examine inter- and intra-network connectivity (Yeo et al. 2011; Power et al. 2013). Children and adolescents with PAE had significantly decreased connectivity compared to unexposed controls in nearly 30% of all possible network interactions (Fig. 2). The somatomotor network had significantly decreased connectivity within itself, as well as with all other networks except the deep gray matter network, suggesting it is significantly affected by PAE. Previous studies have observed lower FA in sensorimotor connections (Lebel et al. 2008), and decreased functional connectivity with sensorimotor areas in children and adolescents with PAE (Long et al. 2018). A small study in infants with PAE showed trend-level decreased functional connectivity between bilateral somatosensory regions (Donald et al. 2016), although another study found the somatosensory network was not affected in children with PAE (Fan et al. 2017). Sensory processing difficulties and gross and fine motor deficits are common in children and adolescents with PAE (Riley and McGee 2005; Jirikowic et al. 2008, 2013; Doney et al. 2014) and may be caused in part by altered brain connectivity in sensorimotor areas.

The ventral attention network also had decreased intra-network connectivity, and decreased connectivity with the default model network and the somatomotor network in children and adolescents with PAE compared to controls. A previous study using independent component analysis found young children with PAE presented decreased intra-network functional connectivity in the ventral attention network (Fan et al. 2017), suggesting an association with this structural finding. Attention deficit is one of the adverse outcomes associated with PAE (Larkby and Day 1997; Jacobson and Jacobson 2002; Riley and McGee 2005; Mattson et al. 2011). Children with PAE present impairment of focusing and shifting attention during cognitive tasks (Mattson et al. 2006; Lane et al. 2014), which might be modulated by the default mode network (Kim 2010; Scheibner et al. 2017). Decreased structural connectivity among those functional networks might underlie attention problems in children with PAE.

In general, network development tends to follow a local-to-global pattern whereby distant regions and networks become more connected with age (Fair et al. 2009; Power et al. 2010; Vogel et al. 2010). The decreased connectivity between networks seen here suggests that children and adolescents with PAE do not show the expected interactions among brain regions (Fair et al. 2012; Rudie et al. 2013; Matthews and Fair 2015; Mevel and Fransson 2016). Previous PAE studies examining individual networks have described reduced functional connectivity in the default mode network (Santhanam et al. 2011), regions within the frontal parietal network and the salience network (Little et al. 2018), and somatomotor networks (Donald et al. 2016; Long et al. 2018). The altered white matter connectivity among networks described here provides a potential structural basis for these observed decreases in functional network integration.

There were several limitations in the current study. Choices of thresholds and parameters to calculate network connectivity with DTI can impact results (Maier-Hein et al. 2017; Sotiropoulos and Zalesky 2017; Sinke et al. 2018). Other sophisticated tractography models such as spherical deconvolution informed filtering of tractograms (SIFT) have been suggested to increase the reproducibility of structural connectome intra-/inter- participants and scans (Smith et al. 2015) and may be useful in future studies. The connectivity matrix here was binarized and unthresholded in order to reduce individual variability and avoid isolated nodes. Future studies may consider alternative methods to build the structural network, such as probabilistic tractography (Cao et al. 2013; Tsai 2018), using weighted connectivity matrix (Cheng et al. 2012), thresholds (Tsai 2018), and/or the integration of multiple DTI metrics to build the edges (Chung et al. 2017), in order to extend our findings. There were no significant results in the group-by-age and group-by-sex interaction analysis. This is likely because the sample sizes provided insufficient power to detect interactions. Furthermore, there were more older children (163 children > 10 years, 77 children ≤ 10 years) than younger children in our study, which may bias results. Future analyses in larger samples are necessary to determine whether there are group-by-age or group-by-sex interactions.

In conclusion, in a large, multi-site dataset, decreased network efficiency, centrality, and intra/inter-network connectivity were observed in the DTI-based structural connectome of children and adolescents with PAE compared with unexposed controls. These results expand previous white matter findings to a network level, suggesting poor network

organization accompanying the white matter deficits in children and adolescents with PAE. Future work should focus on the relationship between the network features and neurobehavioral outcomes, providing a better understanding of the neural basis associated with PAE.

Acknowledgements We thank Brandon Craig for his help on data analysis. This work was supported by grants from the Alberta Children's Hospital Research Institute (ACHRI), the Women's and Children's Health Research Institute (WCHRI), Canadian Institutes of Health Research (CIHR) and the Kid's Brain Health Network (KBHN). Salary support was provided by the University of Calgary I3T program (XL), CIHR (CL), WCHRI and Brain Canada (GL), and AIHS and Canada Research Chairs (CB).

Compliance with ethical standards

Conflict of interest The authors have no financial interests or potential conflicts of interest.

References

Achard S, Bullmore E (2007) Efficiency and cost of economical brain functional networks. PLoS Comput Biol 3:0174–0183. https://doi.org/10.1371/journal.pcbi.0030017

Bassett DS, Bullmore E (2006) Small-world brain networks. Neuroscience 12:512–523. https://doi.org/10.1177/1073858406293182

Baum GL, Ciric R, Roalf DR et al (2017) Modular segregation of structural brain networks supports the development of executive function in youth. Curr Biol 27:1561–1572.e8. https://doi.org/10.1016/j.cub.2017.04.051

Buckner RL, Sepulcre J, Talukdar T et al (2009) Cortical hubs revealed by intrinsic functional connectivity: mapping, assessment of stability, and relation to Alzheimer's disease. J Neurosci 29:1860–1873. https://doi.org/10.1523/JNEUROSCI.5062-08.2009

Bullmore E, Sporns O (2009) Complex brain networks: graph theoretical analysis of structural and functional systems. Nat Rev Neurosci 10:186–198. https://doi.org/10.1038/nrn2575

Cao Q, Shu N, An L et al (2013) Probabilistic diffusion tractography and graph theory analysis reveal abnormal white matter structural connectivity networks in drug-naive boys with attention deficit/hyperactivity disorder. J Neurosci 33:10676–10687. https://doi.org/10.1523/JNEUROSCI.4793-12.2013

Chen Z, Liu M, Gross DW, Beaulieu C (2013) Graph theoretical analysis of developmental patterns of the white matter network. Front Hum Neurosci 7:1–13. https://doi.org/10.3389/fnhum.2013.00716

Cheng H, Wang Y, Sheng J et al (2012) Characteristics and variability of structural networks derived from diffusion tensor imaging. Neuroimage 61:1153–1164. https://doi.org/10.1016/j.immuni.2010.12.017.Two-stage

Chudley AE, Conry J, Cook JL et al (2005) Fetal alcohol spectrum disorder: Canadian guidelines for diagnosis. CMAJ 172:S1–S21. https://doi.org/10.1503/cmaj.1040302

Chung MK, Hanson JL, Adluru N et al (2017) Integrative structural brain network analysis in diffusion tensor imaging. Brain Connect 7:331–346. https://doi.org/10.1089/brain.2016.0481

Dimond D, Ishaque A, Chenji S et al (2017) White matter structural network abnormalities underlie executive dysfunction in amyotrophic lateral sclerosis. Hum Brain Mapp 38:1249–1268. https://doi.org/10.1002/hbm.23452

Donald KA, Eastman E, Howells FM et al (2015) Neuroimaging effects of prenatal alcohol exposure on the developing human brain: a magnetic resonance imaging review. Acta Neuropsychiatr 27:251–269. https://doi.org/10.1017/neu.2015.12

Donald KA, Ipser JC, Howells FM et al (2016) Interhemispheric functional brain connectivity in neonates with prenatal alcohol exposure: preliminary findings. Alcohol Clin Exp Res 40:113–121. https://doi.org/10.1111/acer.12930

Doney R, Lucas BR, Jones T et al (2014) Fine motor skills in children with prenatal alcohol exposure or fetal alcohol spectrum disorder. J Dev Behav Pediatr 35:598–609. https://doi.org/10.1097/DBP.0000000000000107

Drew PD, Kane CJM (2015) Fetal alcohol spectrum disorders and neuroimmune changes

Fair DA, Cohen AL, Dosenbach NUF et al (2008) The maturing architecture of the brain's default network. Proc Natl Acad Sci 105:4028–4032. https://doi.org/10.1073/pnas.0800376105

Fair DA, Cohen AL, Power JD et al (2009) Functional brain networks develop from a "local to distributed" organization. PLoS Comput Biol 5:14–23. https://doi.org/10.1371/journal.pcbi.1000381

Fair DA, Bathula D, Nikolas MA, Nigg JT (2012) Distinct neuropsychological subgroups in typically developing youth inform heterogeneity in children with ADHD. Proc Natl Acad Sci 109:6769–6774. https://doi.org/10.1073/pnas.1115365109

Fan J, Meintjes EM, Molteno CD et al (2015) White matter integrity of the cerebellar peduncles as a mediator of effects of prenatal alcohol exposure on eyeblink conditioning. Hum Brain Mapp 36:2470–2482. https://doi.org/10.1002/hbm.22785

Fan J, Taylor PA, Jacobson SW et al (2017) Localized reductions in resting-state functional connectivity in children with prenatal alcohol exposure. Hum Brain Mapp 38:5217–5233. https://doi.org/10.1002/hbm.23726

Fornito A, Zalesky A, Breakspear M (2015) The connectomics of brain disorders. Nat Rev Neurosci 16:159–172. https://doi.org/10.1038/nrn3901

Fryer SL, Schweinsburg BC, Bjorkquist OA et al (2009) Characterization of white matter microstructure in fetal alcohol spectrum disorders. Alcohol Clin Exp Res 33:514–521. https://doi.org/10.1111/j.1530-0277.2008.00864.x

Gong G, He Y, Concha L et al (2009) Mapping anatomical connectivity patterns of human cerebral cortex using in vivo diffusion tensor imaging tractography. Cereb Cortex 19:524–536. https://doi.org/10.1093/cercor/bhn102

Green CR, Lebel C, Rasmussen C et al (2013) Diffusion tensor imaging correlates of saccadic reaction time in children with fetal alcohol spectrum disorder. Alcohol Clin Exp Res 37:1499–1507. https://doi.org/10.1111/acer.12132

Hagmann P, Cammoun L, Gigandet X et al (2008) Mapping the structural core of human cerebral cortex. PLoS Biol 6:1479–1493. https://doi.org/10.1371/journal.pbio.0060159

Hermundstad AM, Bassett DS, Brown KS et al (2013) Structural foundations of resting-state and task-based functional connectivity in the human brain. Proc Natl Acad Sci USA 110:6169–6174. https://doi.org/10.1073/pnas.1219562110

Honey CJ, Honey CJ, Sporns O et al (2009) Predicting human resting-state functional connectivity from structural connectivity. Proc Natl Acad Sci USA 106:2035–2040. https://doi.org/10.1073/pnas.0811168106

Honey CJ, Thivierge J, Sporns O (2010) Can structure predict function in the human brain ? Neuroimage 52:766–776. https://doi.org/10.1016/j.neuroimage.2010.01.071

Horn A, Ostwald D, Reisert M, Blankenburg F (2014) The structural–functional connectome and the default mode network of the human brain. Neuroimage 102:142–151. https://doi.org/10.1016/J.NEUROIMAGE.2013.09.069

Huang H, Shu N, Mishra V et al (2015) Development of human brain structural networks through infancy and childhood. Cereb Cortex 25:1389–1404. https://doi.org/10.1093/cercor/bht335

Humphries MD, Gurney K, Prescott TJ (2006) The brainstem reticular formation is a small-world, not scale-free, network. Proc Biol Sci 273:503–511. https://doi.org/10.1098/rspb.2005.3354

Iturria-Medina Y, Canales-Rodríguez EJ, Melie-García L et al (2007) Characterizing brain anatomical connections using diffusion weighted MRI and graph theory. Neuroimage 36:645–660. https://doi.org/10.1016/j.neuroimage.2007.02.012

Iturria-Medina Y, Sotero RC, Canales-Rodríguez EJ et al (2008) Studying the human brain anatomical network via diffusion-weighted MRI and graph theory. Neuroimage 40:1064–1076. https://doi.org/10.1016/j.neuroimage.2007.10.060

Jacobson JL, Jacobson SW (2002) Effects of prenatal alcohol exposure on child development. Alcohol Res Health 26:282–286. https://doi.org/10.1111/acer.12395

Jarmasz JS, Basalah DA, Chudley AE, Del Bigio MR (2017) Human brain abnormalities associated with prenatal alcohol exposure and fetal alcohol spectrum disorder. J Neuropathol Exp Neurol 76:813–833. https://doi.org/10.1093/jnen/nlx064

Jenkinson M, Smith S (2001) A global optimisation method for robust affine registration of brain images. Med Image Anal 5:143–156

Jenkinson M, Bannister P, Brady M, Smith S (2002) Improved optimization for the robust and accurate linear registration and motion correction of brain images. Neuroimage 17:825–841

Jenkinson M, Beckmann CF, Behrens TEJ et al (2012) FSL Neuroimage 62:782–790. https://doi.org/10.1016/j.neuroimage.2011.09.015

Jirikowic T, Olson HC, Kartin D (2008) Sensory processing, school performance, and adaptive behavior of young school-age children with fetal alcohol spectrum disorders. Phys Occup Ther Pediatr 28:117–136. https://doi.org/10.1080/01942630802031800

Jirikowic TL, McCoy SW, Lubetzky-Vilnai A, et al (2013) Sensory control of balance: a comparison of children with fetal alcohol spectrum disorders to children with typical development. J Popul Ther Clin Pharmacol = J la thérapeutique des Popul la pharamcologie Clin 20:e212–28

Kim H (2010) Dissociating the roles of the default-mode, dorsal, and ventral networks in episodic memory retrieval. Neuroimage 50:1648–1657. https://doi.org/10.1016/j.neuroimage.2010.01.051

Lane KA, Stewart J, Fernandes T et al (2014) Complexities in understanding attentional functioning among children with fetal alcohol spectrum disorder. Front Hum Neurosci. https://doi.org/10.3389/fnhum.2014.00119

Lange S, Probst C, Gmel G et al (2017a) Global prevalence of fetal alcohol spectrum disorder among children and youth: a systematic review and meta-analysis. JAMA Pediatr 171:948–956. https://doi.org/10.1001/jamapediatrics.2017.1919

Lange S, Rovet J, Rehm J, Popova S (2017b) Neurodevelopmental profile of fetal alcohol spectrum disorder: a systematic review. BMC Psychol 5:1–12. https://doi.org/10.1186/s40359-017-0191-2

Larkby C, Day N (1997) The effects of prenatal alcohol exposure. Alcohol Heal Res World 21:192–198

Lebel C, Rasmussen C, Wyper K et al (2008) Brain diffusion abnormalities in children with fetal alcohol spectrum disorder. Alcohol Clin Exp Res 32:1732–1740. https://doi.org/10.1111/j.1530-0277.2008.00750.x

Lebel C, Rasmussen C, Wyper K et al (2010) Brain microstructure is related to math ability in children with fetal alcohol spectrum disorder. Alcohol Clin Exp Res 34:354–363. https://doi.org/10.1111/j.1530-0277.2009.01097.x

Lebel C, Roussotte F, Sowell ER (2011) Imaging the impact of prenatal alcohol exposure on the structure of the developing human brain. Neuropsychol Rev 21:102–118. https://doi.org/10.1007/s11065-011-9163-0

Leemans A, Jeurissen B, Sijbers J, Jones D (2009) ExploreDTI: a graphical toolbox for processing, analyzing, and visualizing diffusion MR data. Proc 17th Sci Meet Int Soc Magn Reson Med 17:3537

Li L, Coles CD, Lynch ME, Hu X (2009) Voxelwise and skeleton-based region of interest analysis of fetal alcohol spectrum disorders in young adults. Hum Brain Mapp 30:3265–3274. https://doi.org/10.1016/j.asieco.2008.09.006.EAST

Li M, Wang J, Liu F et al (2015) Handedness- and brain size-related efficiency differences in small-world brain networks: a resting-state functional magnetic resonance imaging study. Brain Connect 5:259–265. https://doi.org/10.1089/brain.2014.0291

Little G, Reynolds J, Beaulieu C (2018) Altered functional connectivity observed at rest in children and adolescents prenatally exposed to alcohol. Brain Connect 8:503–515. https://doi.org/10.1089/brain.2017.0572

Long X, Little G, Beaulieu C, Lebel C (2018) Sensorimotor network alterations in children and youth with prenatal alcohol exposure. Hum Brain Mapp 39:2258–2268. https://doi.org/10.1002/hbm.24004

Ma X, Coles CD, Lynch ME et al (2005) Evaluation of corpus callosum anisotropy in young adults with fetal alcohol syndrome according to diffusion tensor imaging. Alcohol Clin Exp Res 29:1214–1222. https://doi.org/10.1097/01.ALC.0000171934.22755.6D

Maier-Hein KH, Neher PF, Houde J-C et al (2017) The challenge of mapping the human connectome based on diffusion tractography. Nat Commun 8:1349. https://doi.org/10.1038/s41467-017-01285-x

Markov N, Ercsey-Ravasz M, Gariel M et al (2011) The tribal networks of the cerebral cortex. In: Chalupa L, Berardi N, Caleo M, et al. (eds) Cerebral plasticity. MIT Press, Cambridge, pp 275–290

Maslov S, Sneppen K (2002) Specificity and stability in topology of protein networks. Science 296:910–913. https://doi.org/10.1126/science.1065103

Matthews M, Fair DA (2015) Research review: functional brain connectivity and child psychopathology—overview and methodological considerations for investigators new to the field. J Child Psychol Psychiatry Allied Discip 56:400–414. https://doi.org/10.1111/jcpp.12335

Mattson SN, Calarco KE, Lang AR (2006) Focused and shifting attention in children with heavy prenatal alcohol exposure. Neuropsychology 20:361–369. https://doi.org/10.1088/1367-2630/15/1/015008.Fluid

Mattson SN, Crocker N, Nguyen TT (2011) Fetal alcohol spectrum disorders: neuropsychological and behavioral features. Neuropsychol Rev 21:81–101. https://doi.org/10.1007/s11065-011-9167-9

Mevel K, Fransson P (2016) The functional brain connectome of the child and autism spectrum disorders. Acta Paediatr Int J Paediatr 105:1024–1035. https://doi.org/10.1111/apa.13484

Moore EM, Migliorini R, Infante MA, Riley EP (2014) Fetal alcohol spectrum disorders: recent neuroimaging findings. Curr Dev Disord Rep 1:161–172. https://doi.org/10.1007/s40474-014-0020-8

Mukherjee RAS, Hollins S, Turk J (2006) Fetal alcohol spectrum disorder: an overview. J R Soc Med 99:298–302. https://doi.org/10.1258/jrsm.99.6.298

Nguyen VT, Chong S, Tieng QM et al (2017) Radiological studies of fetal alcohol spectrum disorders in humans and animal models: an updated comprehensive review. Magn Reson Imaging 43:10–26. https://doi.org/10.1016/j.mri.2017.06.012

Norman A, Crocker N, Mattson S, Riley E (2009) Neuroimaging and fetal alcohol spectrum disorders. Dev Disabil Res Rev 15:209–217. https://doi.org/10.1002/ddrr.72.Neuroimaging

Paolozza A, Treit S, Beaulieu C, Reynolds JN (2017) Diffusion tensor imaging of white matter and correlates to eye movement control and psychometric testing in children with prenatal alcohol exposure. Hum Brain Mapp 38:444–456. https://doi.org/10.1002/hbm.23371

Park HJ, Friston K (2013) Structural and functional brain networks: from connections to cognition. Science (80-). https://doi.org/10.1126/science.1238411

Popova S, Lange S, Probst C et al (2017) Estimation of national, regional, and global prevalence of alcohol use during pregnancy and fetal alcohol syndrome: a systematic review and meta-analysis. Lancet Glob Heal 5:e290–e299. https://doi.org/10.1016/S2214-109X(17)30021-9

Power JD, Fair DA, Schlaggar BL, Petersen SE (2010) The development of human functional brain networks. Neuron 67:735–748. https://doi.org/10.1016/j.neuron.2010.08.017

Power JD, Schlaggar BL, Lessov-Schlaggar CN, Petersen SE (2013) Evidence for hubs in human functional brain networks. Neuron 79:798–813. https://doi.org/10.1016/j.neuron.2013.07.035

Rasmussen C, Andrew G, Zwaigenbaum L, Tough S (2008) Neurobehavioural outcomes of children with fetal alcohol spectrum disorders: a Canadian perspective. Paediatr Child Health 13:185–191

Rasmussen C, Tamana S, Baugh L et al (2013) Neuropsychological impairments on the NEPSY-II among children with FASD. Child Neuropsychol 19:337–349. https://doi.org/10.1080/09297049.2012.658768

Reynolds JN, Weinberg J, Clarren S et al (2011) Fetal alcohol spectrum disorders: gene-environment interactions, predictive biomarkers, and the relationship between structural alterations in the brain and functional outcomes. Semin Pediatr Neurol 18:49–55. https://doi.org/10.1016/j.spen.2011.02.006

Riley EP, McGee CL (2005) Fetal alcohol spectrum disorders: an overview with emphasis on changes in brain and behavior. Exp Biol Med (Maywood) 230:357–365

Riley EP, McGee CL, Sowell ER (2004) Teratogenic effects of alcohol: a decade of brain imaging. Am J Med Genet 127C:35–41. https://doi.org/10.1002/ajmg.c.30014

Riley EP, Infante MA, Warren KR et al (2011) Fetal alcohol spectrum disorders: an cverview. Neuropsychol Rev 21:73–80. https://doi.org/10.1007/s11065-011-9166-x.Fetal

Roos A, Fouche J-P, Ipser J, et al (2018) Structural and functional brain network connectivity in prenatal alcohol exposed neonates as assessed by multimodal brain imaging. In: 41st Annual Scientific Meeting of the Research Society on Alcoholism. San Diego, California

Rorden C, Brett M (2000) Stereotaxic display of brain lesions. Behav Neurol 12:191–200

Rubinov M, Sporns O (2010) Complex network measures of brain connectivity: uses and interpretations. Neuroimage 52:1059–1069. https://doi.org/10.1016/j.neuroimage.2009.10.003

Rudie JD, Brown JA, Beck-Pancer D et al (2013) Altered functional and structural brain network organization in autism. NeuroImage Clin 2:79–94. https://doi.org/10.1016/j.nicl.2012.11.006

Santhanam P, Coles CD, Li Z et al (2011) Default mode network dysfunction in adults with prenatal alcohol exposure. Psychiatry Res Neuroimaging 194:354–362. https://doi.org/10.1016/j.pscychresns.2011.05.004

Scheibner HJ, Bogler C, Gleich T et al (2017) Internal and external attention and the default mode network. Neuroimage 148:381–389. https://doi.org/10.1016/j.neuroimage.2017.01.044

Sidlauskaite J, Caeyenberghs K, Sonuga-Barke E et al (2015) Whole-brain structural topology in adult attention-deficit/hyperactivity disorder: preserved global—disturbed local network organization. NeuroImage Clin 9:506–512. https://doi.org/10.1016/j.nicl.2015.10.001

Sinke MRT, Otte WM, Christiaens D et al (2018) Diffusion MRI-based cortical connectome reconstruction: dependency on tractography procedures and neuroanatomical characteristics. Brain Struct Funct 223:2269–2285. https://doi.org/10.1007/s00429-018-1628-y

Skudlarski P, Jagannathan K, Calhoun VD et al (2008) Measuring brain connectivity: diffusion tensor imaging validates resting state temporal correlations. Neuroimage 43:554–561. https://doi.org/10.1016/j.neuroimage.2008.07.063

Smith RE, Tournier JD, Calamante F, Connelly A (2015) The effects of SIFT on the reproducibility and biological accuracy of the structural connectome. Neuroimage 104:253–265. https://doi.org/10.1016/j.neuroimage.2014.10.004

Sotiropoulos SN, Zalesky A (2017) Building connectomes using diffusion MRI: Why, how and but. NMR Biomed. https://doi.org/10.1002/nbm.3752

Sowell ER, Johnson A, Kan E et al (2008) Mapping white matter integrity and neurobehavioral correlates in children with fetal alcohol spectrum disorders. J Neurosci 28:1313–1319. https://doi.org/10.1523/JNEUROSCI.5067-07.2008

Treit S, Lebel C, Baugh L et al (2013) Longitudinal MRI reveals altered trajectory of brain development during childhood and adolescence in fetal alcohol spectrum disorders. J Neurosci 33:10098–10109. https://doi.org/10.1523/JNEUROSCI.5004-12.2013

Treit S, Zhou D, Lebel C et al (2014) Longitudinal MRI reveals impaired cortical thinning in children and adolescents prenatally exposed to alcohol. Hum Brain Mapp 35:4892–4903. https://doi.org/10.1002/hbm.22520

Treit S, Zhou D, Chudley AE et al (2016) Relationships between head circumference, brain volume and cognition in children with prenatal alcohol exposure. PLoS ONE 11:1–15. https://doi.org/10.1371/journal.pone.0150370

Treit S, Chen Z, Zhou D et al (2017) Sexual dimorphism of volume reduction but not cognitive deficit in fetal alcohol spectrum disorders: a combined diffusion tensor imaging, cortical thickness and brain volume study. NeuroImage Clin 15:284–297. https://doi.org/10.1016/j.nicl.2017.05.006

Tsai S-Y (2018) Reproducibility of structural brain connectivity and network metrics using probabilistic diffusion tractography. Sci Rep 8:11562. https://doi.org/10.1038/s41598-018-29943-0

Tzourio-Mazoyer N, Landeau B, Papathanassiou D et al (2002) Automated anatomical labeling of activations in SPM using a macroscopic anatomical parcellation of the MNI MRI single-subject brain. Neuroimage 15:273–289. https://doi.org/10.1006/nimg.2001.0978

Vogel AC, Power JD, Petersen SE, Schlaggar BL (2010) Development of the brain's functional network architecture. Neuropsychol Rev 20:362–375. https://doi.org/10.1007/s11065-010-9145-7

Wang J, Zuo X-N, He Y (2010) Graph-based network analysis of resting-state functional MRI. Front Syst Neurosci 4:1–14. https://doi.org/10.3389/fnsys.2010.00016

Wang J, Wang X, Xia M et al (2015) GRETNA: a graph theoretical network analysis toolbox for imaging connectomics. Front Hum Neurosci 9:386. https://doi.org/10.3389/fnhum.2015.00386

Watts DJ, Strogatz SH (1998) Collective dynamics of 'small-world' networks. Nature 393:440–442. https://doi.org/10.1038/30918

Wozniak JR, Muetzel RL (2011) What does diffusion tensor imaging reveal about the brain and cognition in fetal alcohol spectrum disorders? Neuropsychol Rev 21:133–147. https://doi.org/10.1007/s11065-011-9162-1

Wozniak JR, Mueller BA, Chang P-N et al (2006) Diffusion tensor imaging in children with fetal alcohol spectrum disorders. Alcohol Clin Exp Res 30:1799–1806. https://doi.org/10.1111/j.1530-0277.2006.00213.x

Wozniak JR, Mueller BA, Bell CJ et al (2013) Global functional connectivity abnormalities in children with fetal alcohol spectrum

disorders. Alcohol Clin Exp Res 37:748–756. https://doi.org/10.1111/acer.12024

Wozniak JR, Mueller BA, Mattson SN et al (2017) Functional connectivity abnormalities and associated cognitive deficits in fetal alcohol Spectrum disorders (FASD). Brain Imaging Behav 11:1432–1445. https://doi.org/10.1007/s11682-016-9624-4

Yan C, Gong G, Wang J et al (2011) Sex- and brain size-related small-world structural cortical networks in young adults: A DTI tractography study. Cereb Cortex 21:449–458. https://doi.org/10.1093/cercor/bhq111

Yeo BTT, Krienen FM, Sepulcre J et al (2011) The organization of the human cerebral cortex estimated by intrinsic functional connectivity. J Neurophysiol 106:1125–1165. https://doi.org/10.1152/jn.00338.2011

Zhang Y, Brady M, Smith S (2001) Segmentation of brain MR images through a hidden Markov random field model and the expectation-maximization algorithm. IEEE Trans Med Imaging 20:45–57. https://doi.org/10.1109/42.906424

Zhao C, Yang L, Xie S et al (2018) Hemispheric module-specific influence of the X chromosome on white matter connectivity: evidence from girls with turner syndrome. Cereb Cortex. https://doi.org/10.1093/cercor/bhy335

Zhou D, Rasmussen C, Pei J et al (2017) Preserved cortical asymmetry despite thinner cortex in children and adolescents with prenatal alcohol exposure and associated conditions. HumBrain Mapp. https://doi.org/10.1002/hbm.23818